Field Spectroradiometer Methods for Remotely Identifying Treeline Vegetation Species: A Case Study Using Limber Pine in Rocky Mountain National Park

Laurel A. Sindewald

Matthew D. Cross

Ted Scambos

Diana F. Tomback

Peter J. Anthamatten

Field Spectroradiometer Methods for Remotely Identifying Treeline Vegetation Species: A Case Study Using Limber Pine in Rocky Mountain National Park

Laurel A. Sindewald, <Laurel.Sindewald@ucdenver.edu>, Department of Integrative Biology, University of Colorado Denver; **Matthew D. Cross**, Department of Environmental Science and Geography, University of Colorado Denver; **Ted Scambos**, Cooperative Institute for Research in Environmental Sciences, University of Colorado Denver; **Diana F. Tomback**, Department of Integrative Biology, University of Colorado Denver; **Peter J. Anthamatten**, Department of Environmental Science and Geography, University of Colorado Denver.

ABSTRACT

Limber pine (*Pinus flexilis)* is an ecologically important conifer in Rocky Mountain National Park (RMNP) that ranges from lower to upper treeline and faces the combined threats of mountain pine beetle (*Dendroctonus ponderosae*) outbreaks, advancing white pine blister rust (*Cronartium ribicola*), and a changing fire regime that could further fragment its metapopulation. As climate warms, limber pine is projected to move upward in elevation into tundra communities. However, the current limber pine distribution at treeline has not been mapped. Here we report groundtruthing methods toward a remote sensing application that might identify the composition of treeline communities by species. First, we used field spectroradiometer methods to characterize intra- and inter-species variation in the spectral reflectance curves of treeline vegetation species. We used photo documentation to connect variation observed in the spectral response to the physical condition of individual trees. We used this field spectroradiometer data to groundtruth WorldView-3 reflectance data toward a future classification of treeline RMNP vegetation.

INTRODUCTION

As a drought-tolerant conifer growing at treeline in Rocky Mountain National Park (RMNP) (Lepper 1980; Steele 1990), limber pine (*Pinus flexilis*) provides a good case study for examining treeline species that may advance under changing climate. Bioclimatic envelope models of limber pine in RMNP predict that its elevational range will move upslope with increasing temperature and precipitation (Monahan et al. 2013). Newer limber pine recruits are infilling treeline communities in RMNP (Sindewald et al. 2020) and limber pine has been observed colonizing at elevations above

bristlecone pine (*Pinus longaeva*) in the White Mountains of eastern California (Millar et al. 2018; Smithers et al. 2018). With warming climate, limber pine may tolerate increasing moisture stress and persist on the drier slopes at treeline east of the Continental Divide in RMNP. However, changes would be difficult to distinguish, because the distribution of limber pine at treeline throughout RMNP is not mapped.

Limber pine's distribution comprises a metapopulation structure throughout the Rocky Mountain region (Peet 1978; Webster and Johnson 2000; Williams 2017). Due to this patchy distribution, limber pine may be vulnerable to local extirpation in the event of a large disturbance, such as

the Cameron Peak and East Troublesome fires in RMNP in 2020. Though the East Troublesome fire burned up to treeline and jumped the Continental Divide, such treeline fire events are still rare. Treeline stands of limber pine may also escape mountain pine beetles (*Dendroctonus ponderosae*), which prefer larger-diameter stems (Maher et al. 2021), and white pine blister rust, which requires high relative humidity for transmission between alternate hosts and pines (Geils et al. 2010; Thoma et al. 2019). Given enough viable seed production, treeline limber pine may allow the species to persist despite these multiple threats. A systematic inventory of where limber pine is found within the treeline ecotone will allow us to determine which non-climatic, abiotic variables are associated with its occurrence, refining distribution modeling for the species under changing climate. Because limber pine grows on steep slopes and sheer cliffs with difficult access, remote sensing provides a tool to improve mapping and identification.

Aerial photography and satellite imagery have long been used to map treeline position across regions and have helped identify the variables that control treeline (Allen and Walsh 1996; Brown et al. 1994; Leonelli et al. 2016; Wei et al. 2020), but individual tree identification was out of reach until sensor technologies improved, providing higher spatial, radiometric, and spectral resolution. By combining airborne hyperspectral imagery and lidar, tree species can be more easily discriminated (Dalponte et al. 2012; Liu et al. 2017; Matsuki et al. 2015; Shen and Cao 2017; Voss and Sugumaran 2008), in some cases with classification accuracies ranging between 76.5% to 93.2% (Dalponte et al. 2012). Nevertheless, these sensors and aircraft overflights are costly. Satellite remote sensing is less costly, but often comes at the cost of decreased spatial resolution. For example, hyperspectral data from space requires a larger spatial resolution (e.g., the Hyperion satellite, with 220 spectral bands but 30 m spatial resolution), because finer spatial resolution sensors have a smaller instantaneous field of view that collects less radiation, so fewer bands can be resolved. Airborne multispectral imagery also yields high classification accuracy (85.8%) (Dalponte et al. 2012), suggesting that a general threshold of spatial and radiometric resolution can be attained that supports species-level tree identification and mapping.

Recently, a high accuracy discrimination between different species of rainforest trees over a managed forest area within the La Selva Research Center in Costa Rica was accomplished using WorldView-3 (WV-3) imagery (Cross et al. 2019a; Cross et al. 2019b). A field spectroradiometer was used to determine the foliage spectral reflectance curves (light reflectance) of in-dividual tree species. The curves were then compared directly with the spectral reflectance curves observed in the WV-3 imagery after atmospheric correction (Cross et al. 2019a). Two spectral vegetation indices specific to WV-3 bands were developed (Cross et al. 2019b) and used to perform an object-based classification on pixel clusters generated by an image segmentation process. This application achieved high classification accuracy (overall accuracies of 75.61% to 85.37%) (Cross et al. 2019a). Prior to this work, applications of WV-3 imagery for species identification had mixed success and the imagery was often used in combination with machine learning or airborne lidar (Immitzer et al. 2012; Li et al. 2015; Majid et al. 2016; Rahman et al. 2018; Wang et al. 2016).

Our ultimate goal is to use the approach demonstrated by Cross et al. (2019a) to identify where limber pine is located across treeline in RMNP, as an input for future species distribution modeling work. The first step is to determine if we can distinguish limber pine among intermixed tree and shrub species in treeline communities across a highly heterogeneous high-elevation landscape. The application to a treeline ecotone introduces new challenges. In contrast to the La Selva Research Station, which is located on a relatively flat area, treeline terrain in RMNP is extremely rugged, requiring substantial corrections for topography. Conversely, imagery of high-elevation areas with thin atmosphere will require little correction for atmospheric effects such as for the high levels of water vapor in a tropical rainforest. Conifers can be reliably distinguished from broadleaf trees, as was recently demonstrated in low-elevation forests using WV-3 and lidar with 94% accuracy (Varin et al. 2020). Classification of conifer species using WV-3 without the expensive addition of lidar overflight data has not been attempted.

Here we present our methods to obtain spectral profiles of six common treeline species. These methods are prerequisites for using WV-3 imagery to ascertain treeline community composition with a focus on determining the presence of limber pine. We adapted Cross et al.'s (2019a) method to obtain *in situ* spectroradiometer data to estimate interspecific variation of six common treeline vegetation species in RMNP and to groundtruth WV-3 reflectance data. We also added additional *in situ* photographic data to support intra-species variation evaluation, acquiring spectra and corresponding photos of different components of a typical treeline tree (e.g., bare sticks, healthy foliage, dry needles). We then compared spectral curves of whole, geolocated tree canopies obtained with the spectrometer to the reflectance curves extracted from corresponding pixels in the WV-3 satellite imagery to groundtruth the selected pixels.

METHODS

WorldView-3 panchromatic and multispectral imagery was purchased in July 2020 from Maxar covering two study areas in Rocky Mountain National Park where limber pine is abundant at treeline: Longs Peak and Battle Mountain. The Longs Peak study area also includes dense willow (*Salix glauca*, *Salix brachycarpa*, and hybrids), Engelmann spruce (*Picea engelmannii*), subalpine fir (*Abies lasiocarpa*), glandular birch (*Betula glandulosa*), and aspen (*Populus tremuloides*). The Battle Mountain study area is mostly composed of limber pine with Engelmann spruce, subalpine fir, willow, and glandular birch as minor components. The WorldView-3 imagery was collected on July 21, 2020 with 0% cloud cover and an off-nadir angle of 16.8 degrees.

We collected ground control points at trail junctions and switchbacks using a Trimble Geo7x centimeter edition geolocator and a Zephyr 2 antennae on a 1 m carbon fiber pole. These ground control points are select landscape features visible in the satellite imagery. MAXAR used the ground control points to perform orthorectification. Atmospheric correction was done using the MAXAR AComp method, which uses cloud, aerosol, water vapor, ice, and snow (CAVIS) band data collected at the same instance as the multispectral data to identify and correct for specific atmospheric influences (Pacifici 2016).

In July and August 2021, we used an Analytical Spectral Devices (ASD) FieldSpec 4 High Resolution Portable Spectroradiometer to collect spectral reflectance data from each dominant vegetation species present at the two sites. We obtained at least 4-5 replicates of each species. We initially collected data at the Longs Peak site on July 2, August 7, and August 12, and at the Battle Mountain site on August 8. However, on these occasions we did point collections with a 13 cm to 16 cm diameter field of view, which resulted in high variability between collections and high intraspecific variability due to differences in proportions of dead needles and stems. So, we adjusted our methodology and collected at the Battle Mountain site again on September 6. In this last collection, we were limited to sampling one individual of each species.

We collected samples within the four-hour period for two hours on either side of local solar noon (approximately 11 am to 3 pm) to ensure adequate illumination. We were restricted in July to a 1-hour collection period before noon due to thunderstorms. Prior to collections, we turned the spectrometer on for 30 minutes to warm up to stabilize temperature and improve sensor accuracy. We calibrated the spectrometer using a Spectralon white reference placed on the scene.

We ensured that the fiberoptic cable was as close to on-nadir as possible to compare with the satellite perspective, and to collect side-scatter while avoiding fore- or back-scatter. In mid-September, we mounted the fiberoptic cable housing to a hiking pole to hold the cable 1.0 m to 1.5 m above the specimen, on-nadir, for a 0.3 m to 0.5 m diameter field of view. For each individual tree, we collected two replicate samples of green needles, brown stems, and two canopy averages acquired by moving the foreoptic field of view slowly across the tree crown area. The moving canopy averages were carefully planned to maintain an on-nadir view and side-scatter collection as the operator carried the fiberoptic cable over the target tree.

We compared the canopy averages to the WorldView-3 reflectance data. To do this, we converted the spectrometer data (hyperspectral, with reflectance values for every nm wavelength between 250 nm to 2500 nm) to equivalent WV-3 bands. We multiplied each reflectance value by the proportion of total radiation the WV-3 multispectral sensor element can detect for that wavelength, then summed the reflectance values across the WV-3 band range.

We used a Trimble GeoXT and a Trimble Geo7x to record perimeters of individual trees corresponding to the September 6th collections. We imported the data to ENVI (version 4.8, Exelis Visual Information Solutions, Boulder, CO) and used the polygons to select pixels that fell entirely within the bounds of the polygons. We exported that data as csv files and compared the median values for each species to the spectrometer canopy averages with a bootstrapped 95% confidence interval (R, version 4.0.5).

RESULTS

The first collections, on July 2, August 7 to 8, and August 12, were highly variable, particularly in the two near infrared bands, and confidence intervals for the median reflectance for each species overlapped across all WV-3-equivalent bands. This was likely due to the small field of view (13 cm to 16 cm), resulting in large differences introduced by variation in plant condition, with differing proportions of dead needles and twigs or pollen cones.

Our collections on September 6, showed that some of the variability can be replicated by comparing green needle collections to brown needle and moving canopy average collections (figures 1-3). The green samples, aside from showing the expected higher reflectance in the green, also
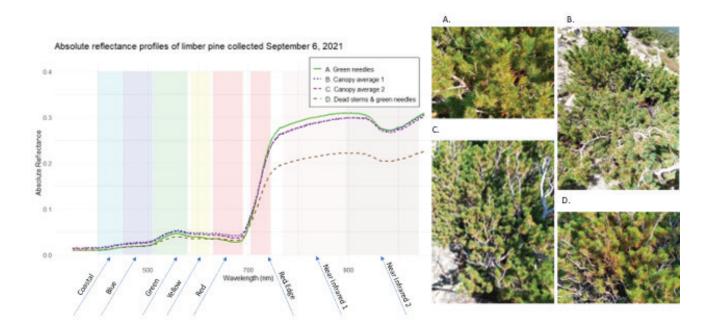
Figure 1. Absolute reflectance profiles of different areas of a krummholz limber pine tree at the Battle Mountain site, collected on September 6, 2021, with an ASD Field Spectroradiometer. Point collections were obtained for green needles and for dead stems and green needles. Moving canopy averages were collected to represent overall variability. The color bands correspond to the wavelength ranges for each of the eight multispectral WV-3 bands. Each labeled collection line in the legend corresponds to a photograph of the sample in the field (A.-D.)
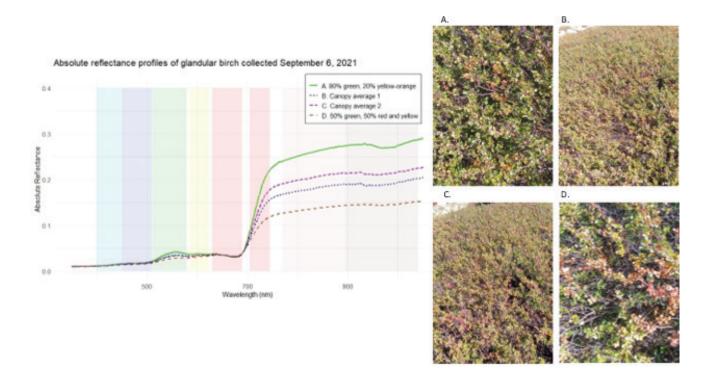

Figure 2. Absolute reflectance profiles of different areas of glandular birch at the Battle Mountain site, collected on September 6. The color bands correspond to the wavelength ranges for each of the eight multispectral WV-3 bands. Each labeled collection line in the legend corresponds to a photograph of the sample in the field.
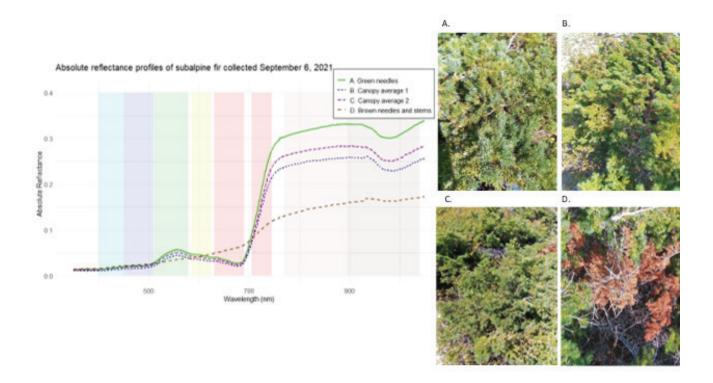
Figure 3. Absolute reflectance profiles of different areas of a krummholz subalpine fir tree at the Battle Mountain site, collected on September 6, 2021. Point collections were obtained for green needles and for dead stems and brown needles. Moving canopy averages were collected to represent overall variability. The color bands correspond to the wavelength ranges for each of the eight multispectral WV-3 bands. Each labeled collection line in the legend corresponds to a photograph of the sample in the field.

showed greater reflectance in both near infrared bands than the samples of brown needles and dead stems. This higher reflectance in the near infrared bands is likely due to water content.
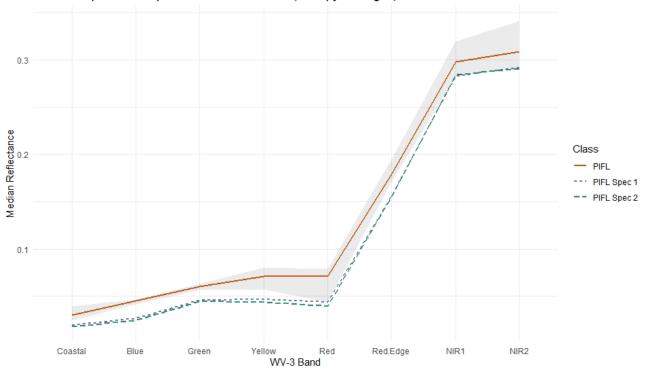
For limber pine, the moving canopy averages were close to the reflectivity values for green needles (figure 1). For glandular birch and subalpine fir, the averages were in between green leaves and dead branches and leaves (figures 2 and 3). By early September, the glandular birch leaves had begun to turn orange and red. Point collections were obtained for an area of mostly green leaves and for an area of mostly red-orange leaves and branches.

The median reflectance values, calculated from the WorldView-3 pixels that fell within the perimeters of the trees or vegetation patches sampled for the spectrometer collections, compared well with the spectrometer reflectance values. The relative difference in reflectance between the bands was mostly consistent between the WV-3 data and the spectrometer data; the shapes of the curves were very close (figures 4 and 5). The absolute reflectance values for each band, however, was greater for the WV-3 data than the spectrometer data.

DISCUSSION

The spectrometer data was successful at groundtruthing the WV-3 imagery, allowing us to compare the training sample data (the reflectance profiles of the pixels in the image for each tree or shrub) to reflectance data collected *in situ*. The spectrometer data also allowed us to demonstrate how each species varied with individual plant condition, useful for interpreting intraspecific variation in reflectance profiles in the satellite imagery. As we attempt a high-resolution satellite imagery classification of the alpine treeline ecotone, field spectrometer data will be invaluable for identifying bands and spectral vegetation indices to discriminate species.

Treeline environments are heterogeneous, with high variability in snow distribution and therefore moisture availability. As plants absorb water, the cytoplasm inside the cell membranes exerts turgor pressure on the cell walls, resulting in structural differences between the cells of plants with greater water content and those of plants that are water stressed. Differences in spectral response due to cell struc-

Figure 4. WorldView-3 median reflectance data from pixels that fell within the perimeters of the limber pine (PIFL) tree from which the spectrometer sample was obtained on September 6. The two spectrometer lines are the two canopy averages from the same individual tree, representing overall canopy variation.

ture can be observed in the near infrared region of the electromagnetic spectrum. Therefore, it is likely that high intra- and interspecific variability will be present in the absolute reflectance response of plants at treeline in the near infrared 1 and near infrared 2 (NIR1 and NIR2) WV-3 bands.

The differences observed in NIR1 and NIR2 bands may therefore not be useful for classifying treeline vegetation species, though a larger sample size is necessary to test this. Species may be separable only in the green and red edge bands, though more spectrometer data using the canopy average method is necessary to estimate intraspecies variation.

Individual trees at treeline are also frequently wind and frost-damaged, leading to high levels of intracanopy variation in spectral reflectance. Much of the variation we observed in our first collections, in July and August, is likely attributable to point collections with a small field of view, capturing only a small portion of the overall canopy variability. Point collections are sensitive to differences in the proportion of green needles and brown needles or stems.

Unfortunately, this means we cannot use the July and August collections.

As the field of view is moved over the canopy, however, the spectrometer will report an average reflectance for the area covered and will thus represent an average of overall intracanopy variation. The moving canopy average will also more closely represent what the WV-3 sensors pick up at 1.24 m resolution. The shape of the median reflectance curve from the WV-3 imagery for a limber pine tree closely resembles the curves obtained for the two canopy averages (figure 4). A departure in curve shape for glandular birch (figure 5) is seen in the red edge and near infrared bands, likely due to deciduous leaf phenology. As the leaves change color and die, the cells collapse and the leaves fall, resulting in a greater proportion of stems and dead leaves in both canopy averages and lower reflectivity in the near infrared.

Collecting moving averages for canopies could allow for the development of spectral libraries for species, representing the variability of species reflectance across the electromagnetic spectrum. A greater representation of in-
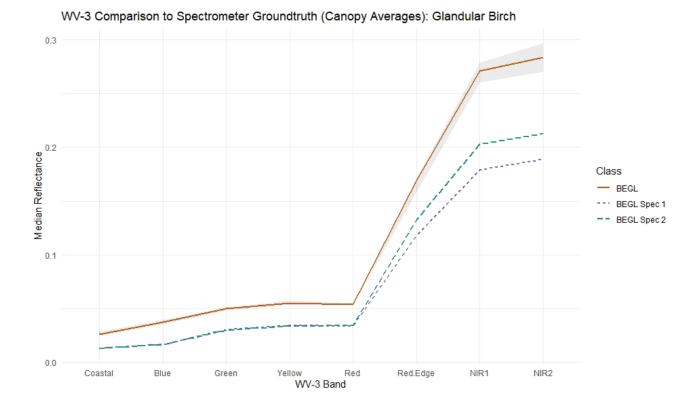
Figure 5. WorldView-3 median reflectance data from pixels that fell within the perimeters of the glandular birch (BEGL) patch from which the spectrometer sample was obtained on September 6. The two spectrometer lines are the two canopy averages from the same patch, representing overall variation.

tra-species variation could then lead to statistical rules for classification of each species on new imagery.

MANAGEMENT IMPLICATIONS

Our paper provides a detailed description of methodology for obtaining an *in-situ* spectral groundtruth of treeline vegetation for imagery classification applications. Spectrometer data provides a spectral groundtruth for training samples identified in the imagery, enabling researchers to determine whether the training pixels identified in the imagery are correctly aligned with objects on the ground. Spectroradiometer groundtruthing may also improve our understanding of the sources of variability that lead to poor classification accuracy, such as variable access to water resources at treeline. Finally, the development of a spectral library of vegetation species, fully representing intraspecies variation over time, may lead to statistical rule sets that could then be used to distinguish species in new locations in new imagery, much as one can use satellite imagery to identify

the probable locations of large mineral deposits of specific types. The rise in availability of affordable, high-resolution satellite imagery may then lead to more efficient monitoring of plant species migration and land cover changes under novel climate scenarios.

ACKNOWLEDGEMENTS

LITERATURE CITED

Allen TR, and SJ Walsh. 1996. Spatial and compositional pattern of alpine treeline, glacier national park, mon-

tana. Photogrammetric engineering and remote sensing 62(11):1261-1268.

Brown DG, DM Cairns, GP Malanson, SJ Walsh, and DR Butler. 1994. Remote sensing and gis techniques for spatial and biophysical analyses of alpine treeline through process and empirical models. United Kingdom: Taylor & Francis Ltd.

Cross M, T Scambos, F Pacifici, O Vargas-Ramirez, R Moreno-Sanchez, and W Marshall. 2019a. Classification of tropical forest tree species using meter-scale image data. Remote Sensing 11(12):1411.

Cross MD, T Scambos, F Pacifici, and WE Marshall. 2019b. Determining effective meter-scale image data and spectral vegetation indices for tropical forest tree species differentiation. IEEE Journal of Selected Topics in Applied Earth Observations and Remote Sensing 12(8):2934-2943.

Dalponte M, L Bruzzone, and D Gianelle. 2012. Tree species classification in the southern alps based on the fusion of very high geometrical resolution multispectral/hyperspectral images and lidar data. Remote Sensing of Environment 123:258-270.

Geils BW, KE Hummer, and RS Hunt. 2010. White pines, ribes, and blister rust: A review and synthesis. Forest Pathol 40(3-4):147-185.

Immitzer M, C Atzberger, and T Koukal. 2012. Tree species classification with random forest using very high spatial resolution 8-band worldview-2 satellite data. Remote Sensing 4(9):2661-2693.

Leonelli G, A Masseroli, and M Pelfini. 2016. The influence of topographic variables on treeline trees under different environmental conditions. Physical Geography 37(1):56-72.

Lepper MG. 1980. Carbon dioxide exchange in pinus flexilis and p. Strobiformis (pinaceae). Madroño 27(1):17-24.

Li D, Y Ke, H Gong, and X Li. 2015. Object-based urban tree species classification using bi-temporal worldview-2 and worldview-3 images. Remote Sensing 7(12):16917-16937.

Liu L, NC Coops, NW Aven, and Y Pang. 2017. Mapping urban tree species using integrated airborne hyperspectral and lidar remote sensing data. Remote Sensing of Environment 200:170-182.

Maher CT, CI Millar, DLR Affleck, RE Keane, A Sala, C Tobalske, AJ Larson, and CR Nelson. 2021. Alpine treeline ecotones are potential refugia for a montane pine species threatened by bark beetle outbreaks. Ecological Applications n/a(n/a):e2274.

Majid IA, ZA Latif, and NA Adnan. 2017. Tree species classification using worldview-3 data. 2016 7th IEEE Control and System Graduate Research Colloquium (ICSGRC); 8-8 Aug. 2016.

Matsuki T, N Yokoya, A Iwasaki. 2015. Hyperspectral tree species classification of Japanese complex mixed forest with the aid of lidar data. IEEE Journal of Selected Topics in Applied Earth Observations and Remote Sensing 8(5):2177-2187.

Millar CI, DA Charlet, DL Delany, JC King, and RD Westfall. 2019. Shifts of demography and growth in limber pine forests of the Great Basin, USA, across 4000 yr of climate variability. Quaternary Research 91(2): 691-704.

Monahan WB, T Cook, F Melton, J Connor, and B Bobowski. 2013. Forecasting distributional responses of limber pine to climate change at management-relevant scales in Rocky Mountain National Park. Plos One. 8(12).

Pacifici F. 2016 Validation of the digitalglobe surface reflectance product. 2016 IEEE International Geoscience and Remote Sensing Symposium (IGARSS); 10-15 July 2016.

Peet RK. 1978. Latitudinal variation in southern Rocky Mountain forests. Journal of Biogeography 5(3):275-289.

Rahman MM, A Robson, and M Bristow. 2018. Exploring the potential of high resolution worldview-3 imagery for estimating yield of mango. Remote Sensing 10(12):1866.

Shen X, and L Cao. 2017. Tree-species classification in subtropical forests using airborne hyperspectral and lidar data. Remote Sensing 9(11):1180.

Sindewald LA, DF Tomback, ER Neumeyer. 2020. Community structure and functional role of limber pine (pinus

flexilis) in treeline communities in Rocky Mountain National Park. Forests 11(8):838.

Smithers BV, MP North, CI Millar, and AM Latimer. 2018. Leap frog in slow motion: Divergent responses of tree species and life stages to climatic warming in Great Basin subalpine forests. Global Change Biology 24(2):E442-E457.

Steele R. 1990. Pinus flexilis James. Silvics of North America. Washington, DC: US Department of Agriculture. p. 348-354.

Thoma DP, EK Shanahan, and KM Irvine. 2019. Climatic correlates of white pine blister rust infection in whitebark pine in the Greater Yellowstone Ecosystem. Forests 10(8):666.

Varin M, B Chalghaf, and G Joanisse. 2020. Object-based approach using very high spatial resolution 16-band worldview-3 and lidar data for tree species classification in a broadleaf forest in Quebec, Canada. Remote Sensing 12(18):3092.

Voss M, and R Sugumaran. 2008. Seasonal effect on tree species classification in an urban environment using hyperspectral data, lidar, and an object-oriented approach. Sensors 8(5):3020-3036.

Wang T, H Zhang, H Lin, and C Fang. 2016. Textural–spectral feature-based species classification of mangroves in Mai Po Nature Reserve from worldview-3 imagery. Remote Sensing 8(1):24.

Webster KL, and EA Johnson. 2000. The importance of regional dynamics in local populations of limber pine (pinus flexilis). Ecoscience 7(2):175-182.

Wei C, DN Karger, and AM Wilson. 2020. Spatial detection of alpine treeline ecotones in the western United States. Remote Sensing of Environment 240:111672.

Williams TJ. 2017. Clark's nutcracker seed use and limber pine metapopulation structure in Rocky Mountain National Park. [Denver, CO]: University of Colorado Denver.